

Fluorescent DNA Nanotags Featuring Covalently Attached Intercalating Dyes: Synthesis, Antibody Conjugation and Intracellular Imaging

Andrea L. Stadler,^{†ℓ} Junriz Delos Santos,^{†,‡} Elizabeth S. Stensrud,[§] Anna Dembska,^{†,‡}
Gloria L. Silva,^{†,‡} Shengpeng Liu,^{†,‡} Nathaniel I. Shank,^{†,‡} Ezgi Kunttas-Tatli,[§] Courtney
J. Sobers,[†] Philipp M. E. Gramlich,[€] Thomas Carell,[€] Linda A. Peteanu,^{†,‡} Brooke M.
McCartney,[§] Bruce A. Armitage^{†,‡*}

Departments of Chemistry[†] and Biological Sciences[§] and Center for Nucleic Acids Science and
Technology[‡], Carnegie Mellon University, 4400 Fifth Avenue, Pittsburgh, PA 15213
Department of Chemistry and Biochemistry, Ludwig Maximilians University, Munich, 81377
Munich, Butenandtstr, 5-13, Haus F, Germany[€]

* Tel: 412-268-4196; Fax: 412-268-1061; e-mail: army@cmu.edu

Abstract: We have synthesized fluorescent DNA duplexes featuring multiple thiazole orange (TO) intercalating dyes covalently attached to the DNA via a triazole linkage. The intercalating dyes stabilize the duplex against thermal denaturation and show bright fluorescence in the green. The emission color can be changed to orange or red by addition of energy-accepting Cy3 or Cy5 dyes attached covalently to the DNA duplex. The dye-modified DNA duplexes were then attached to a secondary antibody for intracellular fluorescence imaging of centrosomes in *Drosophila* embryos. Bright fluorescent foci were observed at the centrosomes in both the donor (TO) and acceptor (Cy5) channels, due to the fact that the energy transfer efficiency is moderate. Monitoring the Cy5 emission channel significantly minimized the background signal due to the large shift in emission wavelength allowed by energy transfer.

ℓ Current address: Biology Department, Brookhaven National Lab, Upton, NY 11973

Synthesis of **TO-N₃-2**.

Synthesis of **TO-Cl-2**. Intermediate **2b** (331.0 mg, 1.00 mmol), was reacted with 3-methyl-2-(methylthio)-1,3-benzothiazol-3-ium iodide (443.0 mg, 1.00 mmol) in 2 mL of anhydrous ethanol and added with triethylamine (139 μ L). It was heated briefly and left overnight at room temperature. The solvent was evaporated under vacuum and the residue washed exhaustively with ethyl ether. The crude dye was purified by column chromatography on silica gel using dichloromethane and 5% methanol in dichloromethane. Fractions were pooled together according to their TLC profile and purified further using the same elution solvent. A total of 77.1 mg (7.4%) of pure **TO-Cl-2** was obtained. ¹H NMR (300 MHz, CDCl₃) δ : 8.56 (d, 1H, J = 8.5 Hz); 8.4 (d, 1H, J = 7.2 Hz); 7.79-7.66 (m, 2H); 7.66-7.57 (m, 2H); 7.40 (ddd, 1H, J = 8.5; 7.2; 1.1 Hz); 7.30-7.11 (m, 3H); 6.60 (s, 1H); 4.66 (br t, 2H, J = 4.22 Hz); 3.96 (br t, 2H, J = 4.42 Hz); 3.90 (s, 3H); 3.67-3.52 (m, 8H). ESIMS (positive mode) m/z : 441.40 (M⁺); calculated for C₂₄H₂₆ClN₂O₂S m/z : 441.14.

The iodo exchange to obtain **TO-I-2** was achieved by dissolving the dye (77.1 mg, 0.14 mmol) in acetone (10 mL), adding sodium iodide (2.0 g, 30 mmol) and refluxing overnight. Progress of the reaction was followed by ESI-MS. The acetone was evaporated and the excess sodium iodide was eliminated by dissolving the dye with dichloromethane and decanting the salt. The dichloromethane was evaporated and the dye was dissolved into a minimum amount of dimethylformamide and added with 91.0 mg (1.4 mmol) of sodium azide. It was stirred at room temperature overnight. The reaction mixture was added with 130 mL of distill water, loaded onto a reversed phase C-18 column and eluted with 1.5 L of distill water (to eliminate the residual solvent and salt) and the dye eluted with 100 mL of methanol containing 0.05% TFA. The counterion was exchanged by adding excess potassium iodide in dry acetone and stand at room temperature overnight. After the evaporation of acetone the dye was extracted with dichloromethane. **TO-N₃-2** was shown to be pure by ¹H NMR, 69.5 mg (0.12 mmol) were recovered (yield 86 %). ¹H NMR (300 MHz, CDCl₃) δ : 8.53 (d, 1H, J = 8.6 Hz); 8.50 (d, 1H, J = 7.4 Hz); 7.91-7.87 (m, 2H); 7.78 (dd, 1H, J = 8.0; 0.9 Hz); 7.72 (ddd, 1H, J = 8.6; 8.4; 2.5 Hz); 7.57 (ddd, 1H, J = 8.6; 7.1; 1.1 Hz); 7.47 (d, 1H, J = 7.1 Hz); 7.42 (br d, 1H, J = 8.6 Hz); 7.38 (br dd, 1H, J = 7.8; 0.9 Hz); 6.78 (s, 1H); 4.78 (t, 2H, J = 4.9 Hz); 4.04 (t, 2H, J = 4.9 Hz); 3.99 (s, 3H); 3.70-3.64 (m, 2H); 3.64-3.58 (m, 4H); 3.34 (t, 2H, J = 4.9 Hz). ESIMS (positive mode) m/z : 448.13 (M⁺); calculated for C₂₄H₂₆N₅O₂S m/z : 448.18.

1. Fluorescence Spectra of TO-Modified DNA Oligonucleotides ODN1-ODN3

The fluorescence spectra for the single-stranded TO-modified DNA strands are shown below. In contrast to the order of fluorescence intensity observed for the *duplexes* (**ODN3** > **ODN1** > **ODN2**), the order of fluorescence for the single strands is **ODN2** > **ODN1** > **ODN3**.

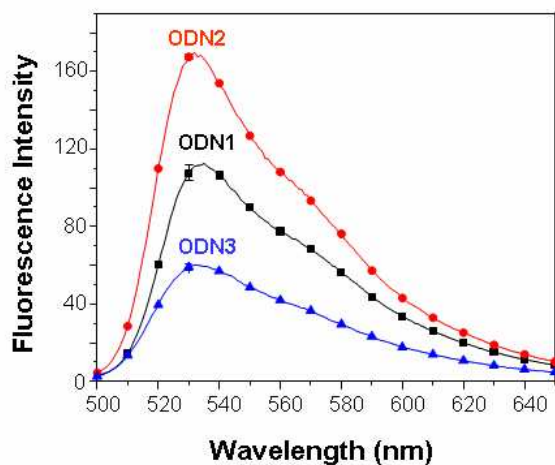
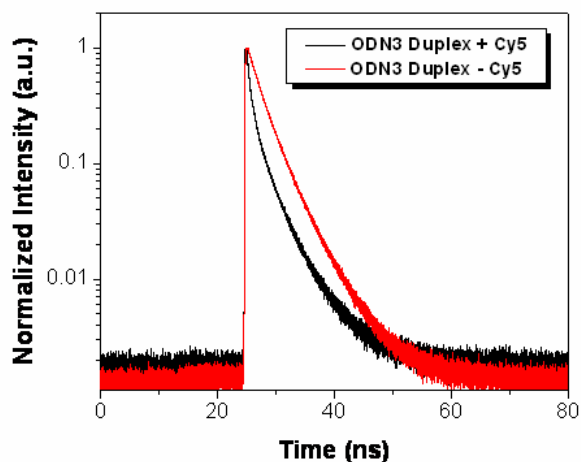


Figure S1. Fluorescence spectra recorded for TO-conjugated DNA strands **ODN1**, **ODN2** and **ODN3**. DNA concentration was 0.1 μ M. 10 mM NaPi (pH 7), 100 mM NaCl and 0.1 mM EDTA. Samples were excited at 485 nm.

2. Fluorescence Lifetime Measurements of TO-Modified ODN3 Duplex \pm Cy5 Acceptor



	ODN3 Duplex – Cy5	ODN3 Duplex + Cy5
A₁	11899.8	5224
t₁	4.4251	3.9774
A₂	16723	8006
t₂	2.0838	1.1222
χ²	1.05	1.44
Weighted Lifetime (ns)	3.057	2.250

Figure S2. Fluorescence lifetimes for **ODN3** duplex recorded in absence or presence of 5'-Cy5 on complementary strand. DNA concentration was 0.1 μ M. Buffer contained 10 mM NaPi (pH 7), 100 mM NaCl and 0.1 mM EDTA. Samples were excited at 450 nm.

3. R₀ Calculation

Following Algar and coworkers, who determined the spectral overlap integral $J = 1.6 \times 10^{-10} \text{ cm}^6$ and using refractive index $n = 1.48$, orientation factor $\kappa^2 = 2/3$, and $\phi_D = 0.2$ (i.e. the fluorescence quantum yield of the donor, TO), we calculate the critical energy transfer distance (R_0) according to the formula:

$$R_0 = [8.79 \times 10^{-28} \text{ mol} \times (n^4 \kappa^2 \phi_D J)^{1/6}] = 40.6 \text{ \AA}$$

This value is significantly greater than that calculated by Algar and coworkers ($R_0 = 26 \text{ \AA}$) due to the larger quantum yield of our covalently attached TO compared with the noncovalently bound TO monocation used in the previous work ($\phi_D = 0.01$).

4. MALDI-TOF Mass Spectrum of ODN4 Single Strand

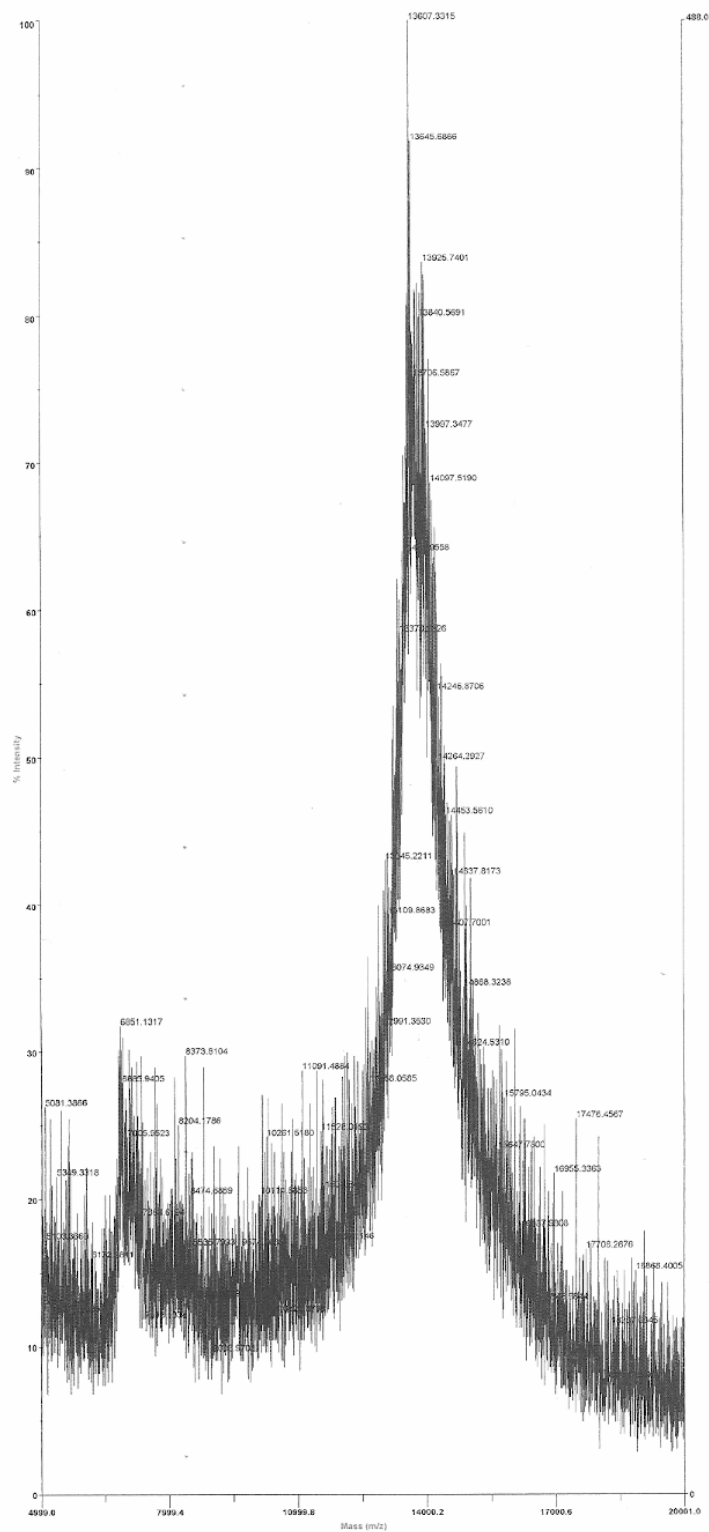


Figure S3. MALDI-TOF mass spectrum of ODN4 single strand. Molecular ion is observed at $m/z = 13,607.3$. (Calculated mass = 13,596.8.)

5. UV-Vis Spectra of ODN4 Single Strand and Duplex

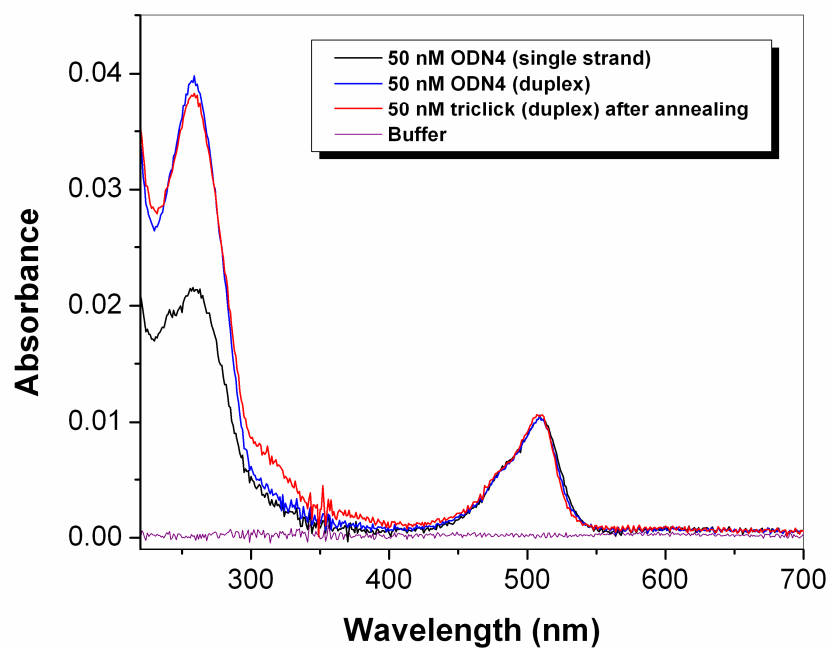


Figure S4. UV-vis spectra of ODN4 single strand and duplex. Samples included 1.0 μ M DNA, 10 mM NaPi (pH 7), 100 mM NaCl and 0.1 mM EDTA.

6. UV Melting Curves of Termolecular Duplexes (X = Uracil-linked TO, Red and Black indicate different strands.)

A termolecular duplex consisting of the three strands shown below was prepared. The red strand was 5'-end-labeled with Cy5. Note that the red and black sequences correspond to different strands.



Two duplexes were prepared. In the first, no TO dyes were attached to the 39mer, meaning three alkynyl-uracil residues were present at the positions labeled "X" in the sequence above. In the second duplex, **TO-N₃-3** was attached to the DNA strand to give a final ratio of 2.4-2.7 dyes per strand. The UV melting curves reflect the stabilizing effect of the TO intercalators. Two transitions are evident in the TO-free duplex: the upper transition at 66.3 °C is assigned to melting of the 19mer strand, due to the significantly higher GC content, leaving the 20mer melting at 53.3 °C. Conjugation of TO dyes to the 39mer strand results in increases in T_m by 5.0 and 7.4 °C. (The corresponding values observed in the absence of the Cy5 label differed by less than 1 °C.)

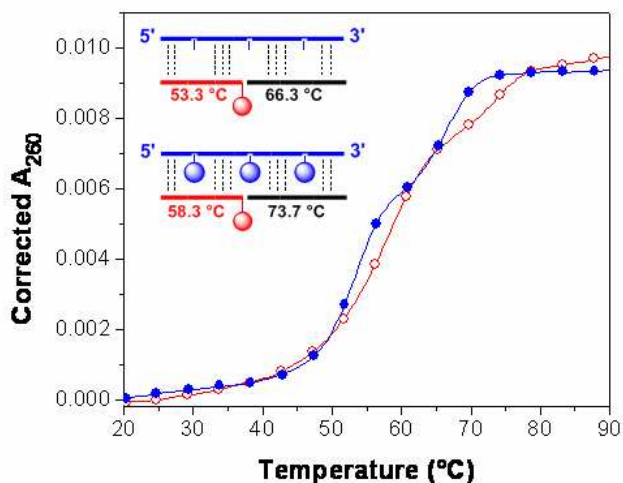


Figure S5. UV melting curves for ternary duplexes shown schematically above. Samples included 1.0 μ M DNA, 10 mM NaPi (pH 7), 100 mM NaCl and 0.1 mM EDTA. Data were corrected by subtracting the initial absorbance at 20 °C from the curve. Intercalation of TO dyes stabilizes both transitions.

7. Spectral Imaging of Individual *Drosophila* Embryos

This figure provides spectral imaging results for individual embryos showing the range of brightness values that are obtained for different embryos. Thus, there is a fluctuation of approximately 10-15% around the mean value (for 31 different embryos), as shown in the lower figure. The similarity in the spectral profiles for the individual embryos indicates that the variation arises from differences in brightness, which is a function of antibody staining efficiency, not FRET efficiency, which would indicate variable hybridization of the triclicked DNA strand to the antibody.

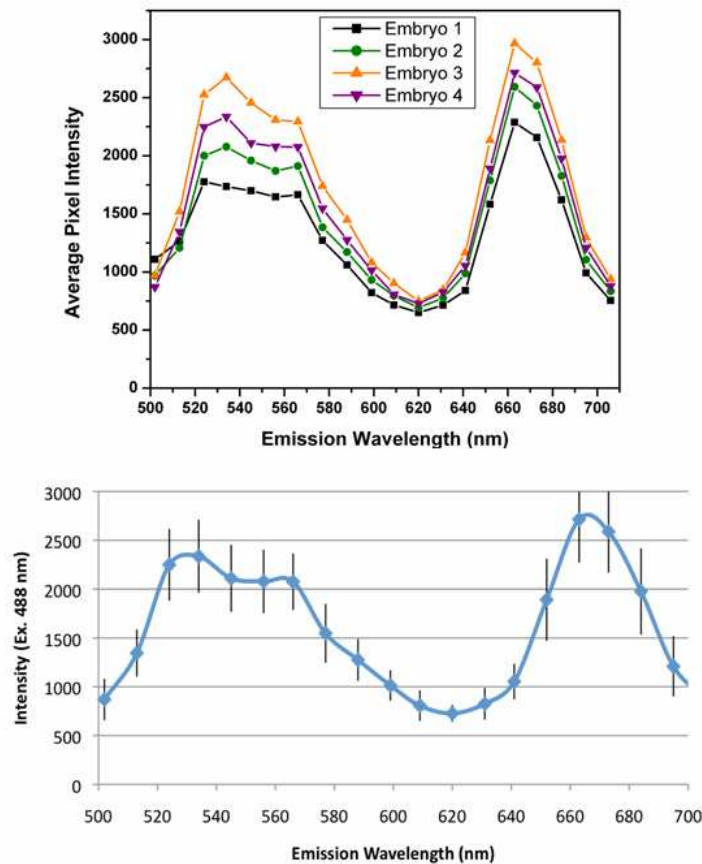


Figure S6. The average pixel intensity at the centrosome of the Ab-nanotag conjugate in 4 different fixed syncytial *Drosophila* embryos. Each point is represented as the average pixel intensity at the centrosome at a given emission wavelength ($n = 30 - 35$ centrosomes per embryo).